

# Optimization of fractional order PI controller to regulate grid voltage connected photovoltaic system based on salp swarm algorithm

Ibrahim Altawil<sup>1,2</sup>, Mohammad Awad Momani<sup>2</sup>, Mahamood A. Al-Tahat<sup>2</sup>, Raed Al Athamneh<sup>3</sup>,  
Mohammed Adnan Al-Saadi<sup>2</sup>, Zaid Albataineh<sup>4</sup>

<sup>1</sup>Faculty of Engineering, Al-Ahliyya Amman University, Amman, Jordan

<sup>2</sup>Department of Electrical Power Engineering, Faculty of Engineering Technology, Yarmouk University, Irbid, Jordan

<sup>3</sup>Department of Industrial Engineering, Faculty of Engineering, The Hashemite University, Zarqa, Jordan

<sup>4</sup>Department Electronics Engineering, Faculty of Engineering Technology, Yarmouk University, Irbid, Jordan

## Article Info

### Article history:

Received Oct 30, 2022

Revised Dec 31, 2022

Accepted Jan 17, 2023

### Keywords:

Fractional order controller

Grid voltage

PI controller

PV system

Salp swarm algorithm

## ABSTRACT

Problems with voltage and stability have arisen as a result of the dramatic development in renewable energy generating units, notably solar energy systems linked to low and medium voltage networks, and the influence of active loads that vary rapidly from time to time during the day. Because reactive power is directly proportional to voltage, its use to renewable energy producing units can only improve their efficiency. Better performance for these controllers is possible via the usage of several controller types. In this paper, we use a salp swarm optimization algorithm (SSA) to design fractional order proportional-integral (FO-PI) controllers, whose job it is to regulate the active and reactive power of solar inverters by compensating for the overvoltage and undervoltage presented by the inverters' ability to absorb and produce reactive power. After that, we compared the FO-PI controller's results to those of the standard PI controller. Grid-connected photovoltaic (PV) system modeling and simulation were performed using the MATLAB/Simulink modeling and simulation tools. After that, the full PV system was simulated in the most likely situations across a range of grid and weather conditions. We may infer from the simulation results that this model is credible, reliable, and applicable to the analysis of grid-connected PV systems.

This is an open access article under the [CC BY-SA](https://creativecommons.org/licenses/by-sa/4.0/) license.



## Corresponding Author:

Zaid Albataineh

Department Electronics Engineering, Faculty of Engineering Technology, Yarmouk University

Shafiq Irshidat st., Irbid, Jordan

Email: zaid.bataineh@yu.edu.jo

## 1. INTRODUCTION

Voltage stability issue has received attention in recent years as the number of renewable distributed generation (DG) units has increased significantly. Solar power system is the most widespread of these sources. Solar systems can linked to low- and medium-voltage networks, which can meet the growing needs for energy in the light of population growth in the short and long term. The voltage instability is an inability to maintain acceptable voltage on all electrical system buses under normal conditions and after the electrical system has been disturbed. A major cause of these disturbances is the sudden change in electrical loads, changing or losses of generation, in addition to the disturbance associated with the flow of the reactive power through transmission lines. The problem of the overvoltage caused by a disturbance in the electrical system can be reduced by controlling the reactive power of distributed grid-tied photovoltaic (PV) inverters. Modern inverters are

equipped with internal P-Q controllers, through which the inverter can generate or consume reactive power, thereby mitigating the increase in voltage within the electrical grid [1], [2].

Bouderres *et al.* [3] and Krishan *et al.* [4] explained the expanding establishment of photovoltaic panels in low-voltage networks causes an overvoltage issue, particularly during high generation and low utilization periods. Reactive power absorption is among the methods followed by both researchers and system operators as an effective solution for overcoming the overvoltage problems. Sharma *et al.* [5] and Huang *et al.* [6] compare three decentralized approaches to network voltage control by controlling the reactive power of PV inverters in terms of their ability to reduce the problem of PV voltage penetration in low-voltage networks. Two of these methods based on the static reactive power supply methods category, according to German code that relates to the distribution generators connected with the LV network, the third way dynamic reactive power controllers used to adjust and maintain network voltage [7].

To enhance voltage regulation at the point of common coupling (PCC), Tehrani *et al.* [8] and Mao *et al.* [9] regulates the reactive power of the PV inverters linked to the network. In order to maximize the total distributed generation (DG) penetration and improve the distribution/transmission network utilization in a typical power grid, optimal power flow (OPF) has been used in conjunction with solar inverter control schemes [10]–[12]. OPF is formulated as an optimization problem based on artificial intelligence algorithms. Several studies [13], [14] have used proportional-integral (PI) controllers to regulate the alternating current (AC) side currents in grid-connected PV systems. Through a voltage control loop, the DC-link voltage is regulated, and the DC voltage error is used by a proportional-integral (PI) controller to provide references for the alternating current (AC) in the stationary (abc or dq) or synchronous (dq) frames [15]–[21]. For this study, the PI controller is employed as a reference point against which the fractional order controllers developed using AI particle swarm optimization techniques may be evaluated. Compared to integer order controllers [22], fractional order controllers, which make advantage of fractional order operators in their designs, are more stable and provide the user greater leeway.

Erol [23] looked at the feasibility of using a fractional order proportional integral derivative (FO-PID) controller for a multi-neutral point (MNP) inverter with three output levels. The FO-PID controller is argued to have great dynamic responsiveness and outstanding start-up response in this work. The resilience and efficiency of the FO-PID controller have been confirmed by experiments. When connecting to the utility grid, a DC/AC converter is required. Reduced harmonic content and other power quality standards need a sophisticated control system in a converter of this kind [24]. A switchable converter is required in certain configurations [25]. Integrating photovoltaic (PV) systems into preexisting utility networks necessitates the use of inverters, and many approaches have been devised for their management. Current and power are two classes of control loop parameters [26]. First to employ an indirect control strategy for active and reactive power was the induction motor's field orientation control (FOC) [27]. Voltage-oriented control describes how the voltage vector is directed relative to the current vector voltage oriented control (VOC). Instead of calculating active and reactive power from input current and voltage measurements of PWM converters, direct power control (DPC) [28] uses hysteresis comparators and a switching table to provide instantaneous power regulation. While DPC's hysteresis controllers allow for great dynamic behavior, the fact that it cannot maintain a constant switching frequency and demands a high sampling rate are two of the primary objections thrown against it [29]. Using VOC and DPC as a foundation, further controls such as virtual flux-based VOC (VFOC) and virtual flow-based DPC (VFDPC) employ virtual flux for voltage estimates [30]. It was proposed by Zeb *et al.* [31] to use a technique called direct power control with vector modulation (DPC-SVM).

To monitor the loop's reference, a PI/PID controller has been implemented. When the controller's settings are adjusted precisely, a steady and dynamic response is achieved [32]. An efficient controller has a positive effect on the control's quality and durability [33]. In order to usher of a new class of controllers known as fractional order PID (FOPID), [34] the integration order in the traditional PID controller was modified to a fractional one. The usage of a FOPID controller results in a controlled system that responds better to specifications and can be adjusted more freely. When compared to a standard PID-controlled system, the reaction time of a system that has had its parameters fine-tuned using FOPID is much faster and more reliable. Altawil *et al.* [35] provide a thorough analysis of the differences between traditional PID controls and FOPID controllers. The FOPID has been employed for flux-oriented virtual control of a PWM rectifier linked to the grid by Albataineh [36]. The simulation findings reveal that fractional order is more robust against changes in load and parameters, while the quality of the injected power is better than that produced with a traditional PID controller. Automatic voltage regulator (AVR) system performance has been greatly enhanced by the introduction of the fractional filter SCA-FOPIDFF controller [37], which was suggested and applied to the FOPID controlling AVR system to increase the responsiveness. Whether the converter's controller is PID or FOPID, tuning its settings is necessary to get a good response. Genetic algorithms, cuckoo search algorithms, chaotic ant swarm algorithms, grey wolf optimization, water cycle algorithms, sine cosine algorithms, gradient-based optimization, and particle swarm optimization [30]–[35], [36]–[42]. The PSO algorithm was selected among those listed for controlling our converter. By modeling the communications of swarming creatures, PSO

constructs a solution to the given issue. The PSO algorithm provides a useful method for solving optimization problems with continuous variables [41]–[45].

To that end, the first two benefits stem from the fact that meta-heuristics (salp optimization technique) examine and solve optimization issues by focusing just on the inputs and outputs [46], [47]. In other words, meta-heuristics see optimization as a black box. As a result, there is no need to compute the derivative of the search space. This makes them very adaptable to a wide variety of challenges. Because meta-heuristics are a kind of stochastic optimization approach, they benefit from random operators. This helps them avoid local solutions while dealing with real-world situations, which often involve a high number of local optima. Because of these benefits, meta-heuristics are used in a variety of fields of research and business.

However, we encompass substantially extended as well as thoroughly revised versions of the thesis in [48]. The objective in this work is to achieve a solution for overvoltage and under voltage issues caused by the on-grid PV systems generation changes in addition to the load changes. In this work salp swarm algorithm (SSA) as an optimization method will be used to design a FO-PI controller that controls reactive power for PV inverters to regulate the grid voltage, maintain and increase the stability of the electrical grid. Moreover, this paper models a grid-connected solar system with an inverter under the direction of current loops. Voltage-oriented control (VOC) is used to regulate the PWM frequency. Traditional PI control has been compared to its modern-day counterpart, the forward-looking PI (FOPI) controller. Our paper's innovation lies in the fact that it employs the SSA algorithm to fine-tune the parameters of the traditional PI and FOPI.

There are six major parts to this study. The system's primary parts are outlined in the section 2. In section 3, we see an illustration of the inverter's modeled behavior and the presented control using a FOPID controller. In section 4, we introduce the salp swarm optimization method and we present and discuss the findings we have gotten in section 5. At last, a summary of the most important points is presented in section 6.

## 2. THE IMPACT OF PV SYSTEMES ON VOLTAGE STABILITY OF ELECTRICAL SYSTEMS

The voltage stability gained significant attention since the number of renewable distributed generation (DG) units has increased in recent years. Excessive PV voltage penetration to the grid during low demand periods could harmfully affect power system operations. This led the need to development a solar inverter, where these inverters have the ability to generate reactive power to mitigate the problems caused by PV voltage penetration. To describe the impact of solar energy systems penetration on the grid voltage, take the simple electrical system in Figure 1.

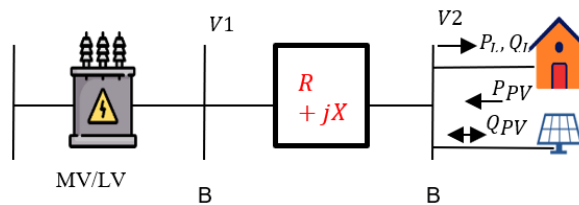


Figure 1. Simple electrical network structure

According to [25], the voltage at  $V_2$  is given by (1).

$$V_2 = V_1 - \frac{(P_L - P_{pv})R + j(Q_L - Q_{pv})X}{V_1} \quad (1)$$

As we can see in (1), when the consumer load is higher than the production of the solar system, this leads to a decrease in voltage along the feeder. Then when the production of the solar system is higher than the load, the excess power flows towards the grid, which leads to a rise voltage as (2).

$$V_2 = V_1 + \frac{(P_{pv} - P_L)R + j(Q_{pv} - Q_L)X}{V_1} \quad (2)$$

The amount of reactive power that can absorb or inject to the grid is decided by the capacity of the solar system. Figure 2 depicts the equivalent circuit of a simple electrical system consisting of a solar system with the grid using the PV inverter. According to [24], one can determine the range of reactive power as (3).

$$-\left(\sqrt{\left(\frac{V_s V_{inv}}{X_i}\right)^2 - (P_s)^2} - \frac{V_s^2}{X_i}\right) \leq Q_s \leq \left(\sqrt{\left(\frac{V_s V_{inv}}{X_i}\right)^2 - (P_s)^2} - \frac{V_s^2}{X_i}\right) \tag{3}$$

Figure 3 depicts the power quality (PQ) curve of the solar inverter, which demonstrates that the inverter is able to generate or absorb reactive power within a limited range ( $Q_{min} < Q < Q_{max}$ ) only when the active power generated  $P_{pv}$  is smaller than the inverter's capacity  $S$ . From the PQ curve in Figure 3, to control the reactive power through PV inverters, which requires flexibility in the power factor range without affecting the normal operation and active power production of the system, in other words, the ability of the inverter to supply or absorb passive power definite by the PF of the inverter. When it is lagging PF,  $Q_{pv}$  is positive, this means that the inverter absorbs reactive power, while when the system is leading PF,  $Q_{pv}$  is negative, this means that PV inverter generates reactive power and injects it into the PCC to support voltage stability.

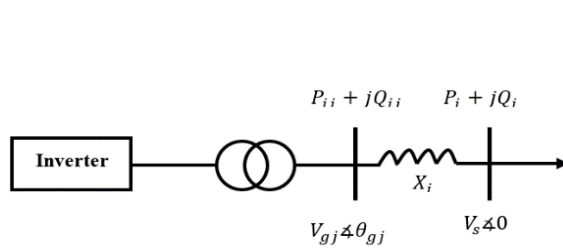


Figure 2. Power plant equivalent circuit

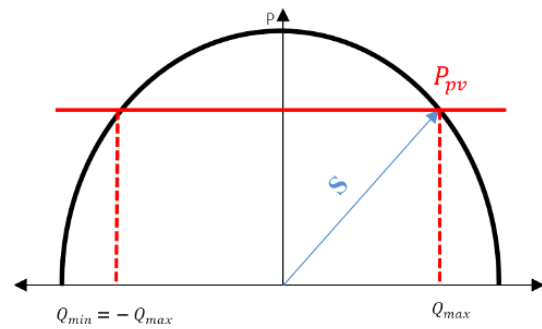


Figure 3. P-Q of the solar inverter

Figure 4 shows the overall trend in the consumption or generation of reference reactive power across a variety of voltage limit violations as shown by the generic *volt – var* curve. The inverter injects reactive power to keep the terminal voltage at the PCC from falling below the minimum acceptable voltage  $V_2$ , and it absorbs reactive power to bring the voltage down if it climbs beyond the maximum allowable voltage  $V_3$ .

In (4), which is readily applied in inverter controllers, uses the *volt – var* curve to determine the amount of reactive power that provides the reference value of reactive power for the PV inverter controllers based on fluctuations in the voltage values at PCC ( $V_{meas}$ ).

$$Q_{pv}^{ref} = \begin{cases} Q_{max} & V_{meas} < V_1 \\ \frac{(V_{meas}-V_1)*Q_{max}}{(V_1-V_2)} & V_1 \leq V_{meas} \leq V_2 \\ 0 & V_2 \leq U_{meas} \leq V_3 \\ \frac{(V_{meas}-V_3)*Q_{max}}{(V-V_4)} & V_3 \leq U_{meas} \leq V_4 \\ -Q_{max} & V_{meas} > V_4 \end{cases} \tag{4}$$

The maximum reactive power is given by (5):

$$Q_{max} = \tan(\cos^{-1}(\cos\theta)) \times P_n \tag{5}$$

where  $P_n$  denotes the PV power capacity of the inverter.

In Figure 5, we see a high-level diagram of a generic power conversion interface suitable for PV systems that are wired into the local utility's electrical grid. The system incorporates a photovoltaic (PV) generator, which may take the form of a single module, a series of modules, or a parallel array of strings. Figure 5(a) represents the lagging power factor scenario and Figure 5(b) represents the leading power factor. A capacitor is often used as a passive input filter after a PV system to isolate the input voltage and current from the subsequent power stages and reduce ripple on the PV side of the power supply. After the input filter, a DC-DC stage may be used to increase the output voltage, perform maximum power point tracking (MPPT), and other functions typical of a PV system. Grid-connected DC-AC converters, also known as PV inverters, are linked to the DC-DC stage (or the input filter if no DC-DC stage is used) as shown in Figure 6. Without a DC-DC stage, a PV system's input filter serves a similar function as a DC-link capacitor.

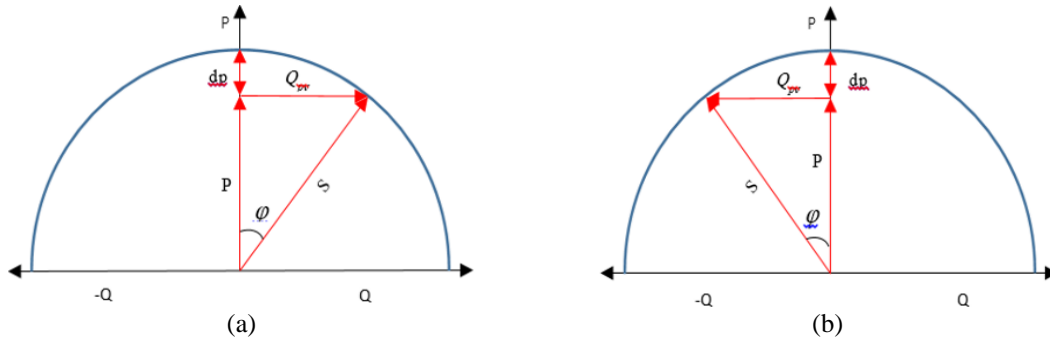


Figure 4. PQ characteristic of solar inverter: (a) lagging power factor and (b) leading power factor

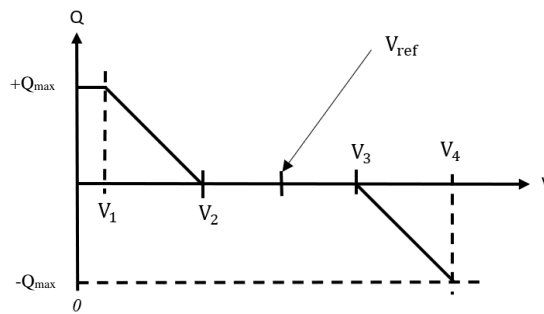


Figure 5. Standard reactive power methods of the generic volt-var curve - Q(V)

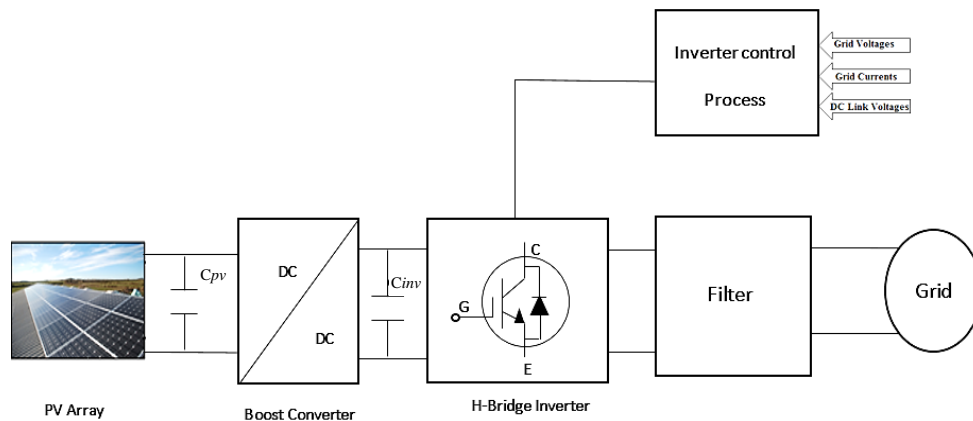


Figure 6. A photovoltaic (PV) system that is hardwired into the grid

### 3. FRACTIONAL ORDER PID CONTROLLERS (FO-PID)

PID controllers considered one of the most prevalent types of controllers in the fields of engineering and control. This diffusion comes because these controllers distinguished by their simplicity of structure, which made them easier for implementing, in addition to the diversity of tuning methods in these controllers. Nevertheless, the FO-PID controller ( $PI^\alpha D^\beta$ ) in Figure 7, is given as (6) and (7).

$$c(t) = \frac{u(t)}{e(t)} = (Kp + Ki D_t^{-\alpha} + Kd D_t^\beta) \alpha, \beta > 0 \tag{6}$$

and

$$C(s) = \frac{U(s)}{E(s)} = Kp + Ki s^{-\alpha} + Kd s^\beta \alpha, \beta > 0 \tag{7}$$

where;  $Kp$  represents the proportional gain;  $Ki$  is the integral gain; and  $Kd$  is derivative gain.

The fractional order PI is given as (8).

$$C(s) = Kp + Ki s^{-\alpha} \quad (8)$$

Fractional order PD controller

$$C(s) = Kp + Kd s^{\beta} \quad (9)$$

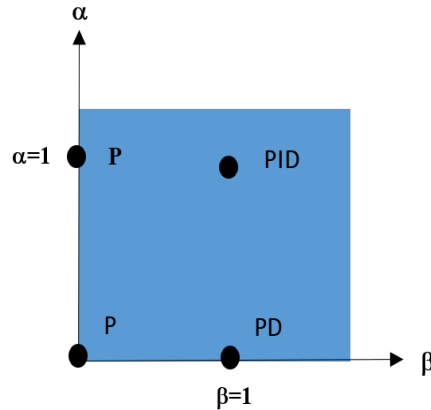


Figure 7. The fractional order PID controller

#### 4. SALP SWARM OPTIMIZATION ALGORITHM

The salp swarm method (SSA) is a new optimization algorithm inspired on salps' swarming process. It was suggested by Mirjalili, S. M. SSA replicates the swarming activity of marine animals called salps when travelling and foraging in the ocean. This algorithm was inspired by natural algorithms, which are widely used approaches due to their ability to avoid the optimum local, as well as their flexibility, simplicity, and capacity to discover a good solution for real-world issues. All of these qualities are inspired by real-world phenomena such as swarming, humans, physics, and so on [6]. They resemble jellyfish in their tissues and motility to search food sources [18]. Figure 8 shows the structure of the single salp. Salps frequently found in swarms known as salp chains, each of which has a leader and a group of followers.

Nevertheless, Figure 8 displays SSA's optimization procedure for resolving the given optimization issue. All salps (search agents) were randomly dispersed around the SSA's predetermined search area. Then, it takes a look at the current salp population to find the most dominant salp and force the others to follow. All procedures, save the startup phase, will be repeated until the stopping condition is met, with the goal of improving salp quality as much as possible. The objective of our research is to determine the optimal values for the controller parameters by using the FOPI parameters as optimization variables in the proposed system model and minimizing an error integrating fitness function (FF).

If we can reduce the error, we can get closer to the optimal options for fine-tuning the FOPI controller. Integral errors that are often used for integrating fitness alternatives include the integral time absolute error (ITAE). It is one of the most popular error integrating fitness function, beating out competitors like the ISE, IAE, and ITSE [45] due to its simplicity and superior performance. Both ISE and ITSE are very abrasive and provide infeasible outcomes because of the squaring of error. In addition, the time multiplying error function is not included in IAE, making it a poor alternative to ITAE since it offers more accurate error indexing [45]. As a consequence, the proposed method makes use of ITAE as the fitness function to maximize the response of the under study system. The fitness function (FF) may be written as follows, based on the ITAE:

$$ITAE = \int_0^{\infty} t |e_v(t)| dt \quad (10)$$

Where  $t$  is the simulated time and  $e_v(t)$  is the error signal, and it is determined by subtracting the voltage at PCC from the reference voltage according to (11).

$$e_v = V_{ref} - V_{PCC} \quad (11)$$

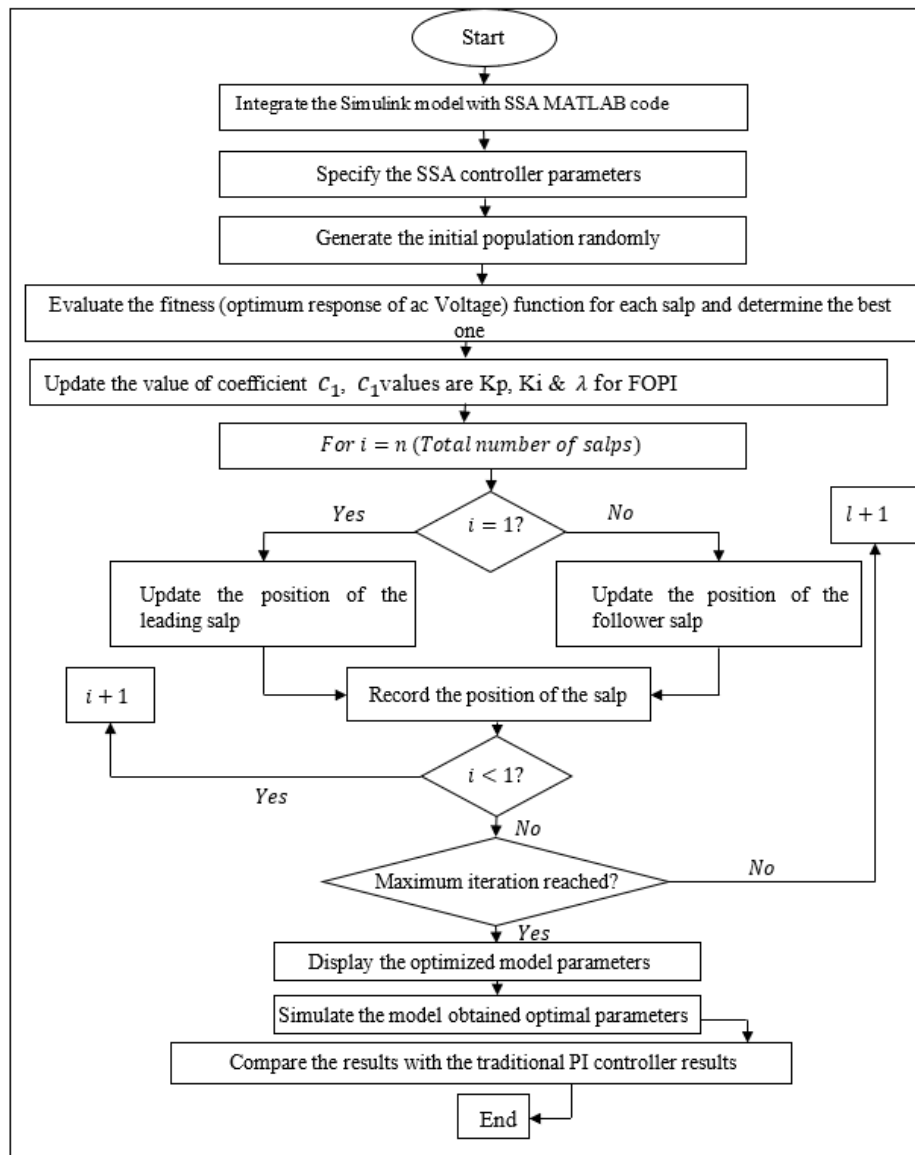


Figure 8. The flow chart of Salp swarm optimization algorithm for FO-PI controller

## 5. SIMULATION RESULTS

Primary PV system components have been simulated and validated for grid integration. The PV array, DC-DC boost converter, VSI, PLL, LCL filter, MPPT controller, and VSI controller are the many parts involved. The produced parts provide the basis for a whole PV system that is linked to the grid. The suggested system was put through its paces in four distinct situations, with varying degrees of weather and grid conditions, and the results were reviewed and debated. Modeling the grid-connected PV system with MATLAB/Simulink, as illustrated in Figure 9.

The PV array: In our work we will use a 100 KW PV system composed of an array containing 27 parallel strings and 17 series connected modules per string. The IV and PV curves for the solar system are respectively presented in Figure 10(a) and Figure 10(b) for different cases of radiation. The PV model having the PV system characteristics presented in Table 1.

In order to determine the optimal duty cycle for the boost converter, the MPPT controller employs the perturb and observe (P&O) method. In order to get the most energy out of the PV system, this controller will adjust the boost converter's duty cycle automatically. The Simulink circuit seen in Figure 11 was used during MPPT algorithm testing. On top of it, the DC-DC boost converter: the intended result of the boost converter is a voltage of 700 volts at the terminals. The specifications of the planned boost converter are listed in Table 2.

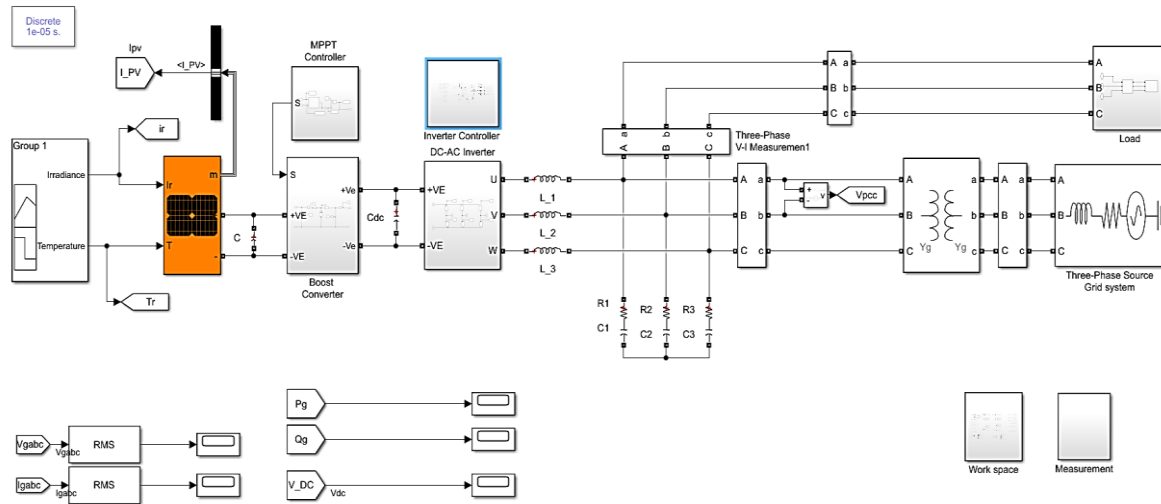


Figure 9. MATLAB model for the grid-connected PV system

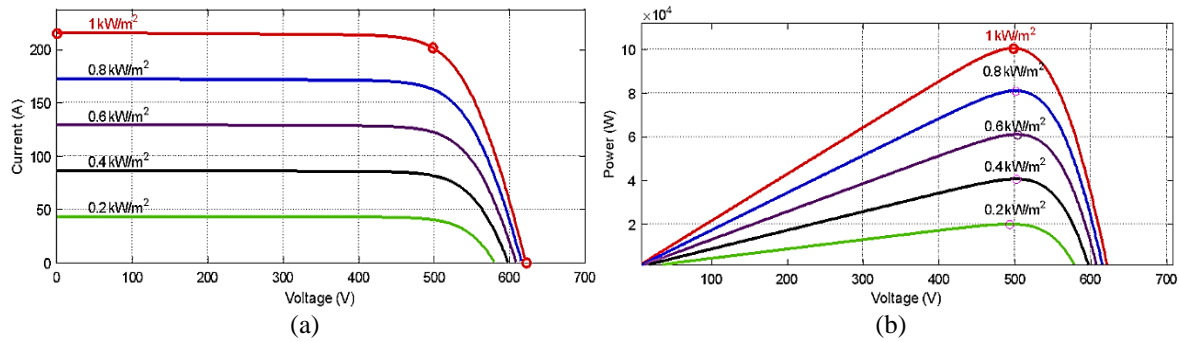


Figure 10. The IV and PV curve for the solar system (a) IV curve and (b) PV curve

Table 1. System characteristics

Characteristic	Value
Maximum power for module (Watt)	218.87
Cell per module	60
Open circuit $V_{oc}$ (volt)	36.6
Short circuit current $I_{sc}$ (Ampere)	7.97
Voltage at maximum power point	29.3
current at maximum power point	7.47
Temperature coefficient of $V_{oc}$ /deg.c	-0.36101
Temperature coefficient of $I_{sc}$ %/deg.c	0.10199

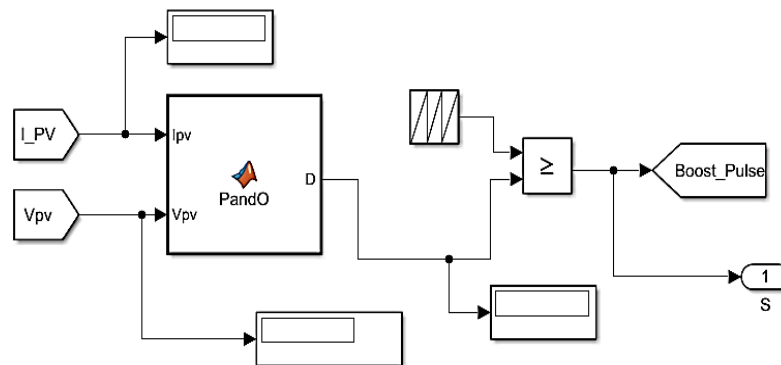


Figure 11. The MATLAB/Simulink circuit of P&O MPPT technique



Table 2. Boost converter parameters values

Parameter	Value
$L$	4.5 mH
$C_{dc}$	5600 $\mu F$
$C_{pv}$	10 $\mu F$
$V_o$	700 volt
$f_{sw}$	10 KHz

The MPPT controller determines the boost converter's duty cycle. Figure 12 depicts the Simulink model of the boost converter. The voltage source inverter (VSI) uses a 3-level IGBT VSI inverter to transform the 700V DC-link voltage into the 400 V L-to-L rms AC voltage utilized by the load. SPWM is used to regulate the inverter switches. The inverter controller is responsible for generating the SPWM signals. The VSI controller is responsible for providing the proper gate signals to the VSI switches, which in turn provide the necessary alternating current (AC) voltages and currents. The VSI controller MATLAB/Simulink model is shown in Figure 13.

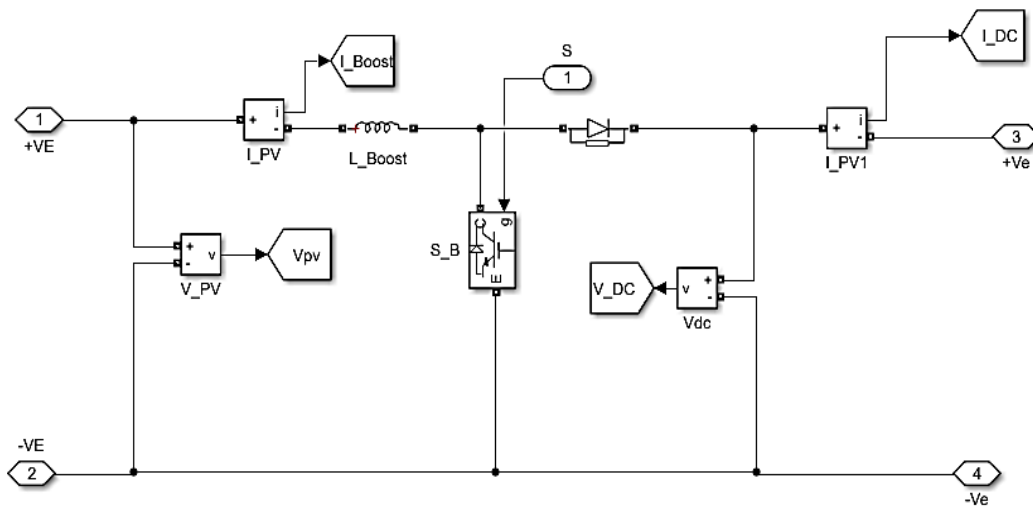


Figure 12. The MATLAB/Simulink circuit of the boost converter

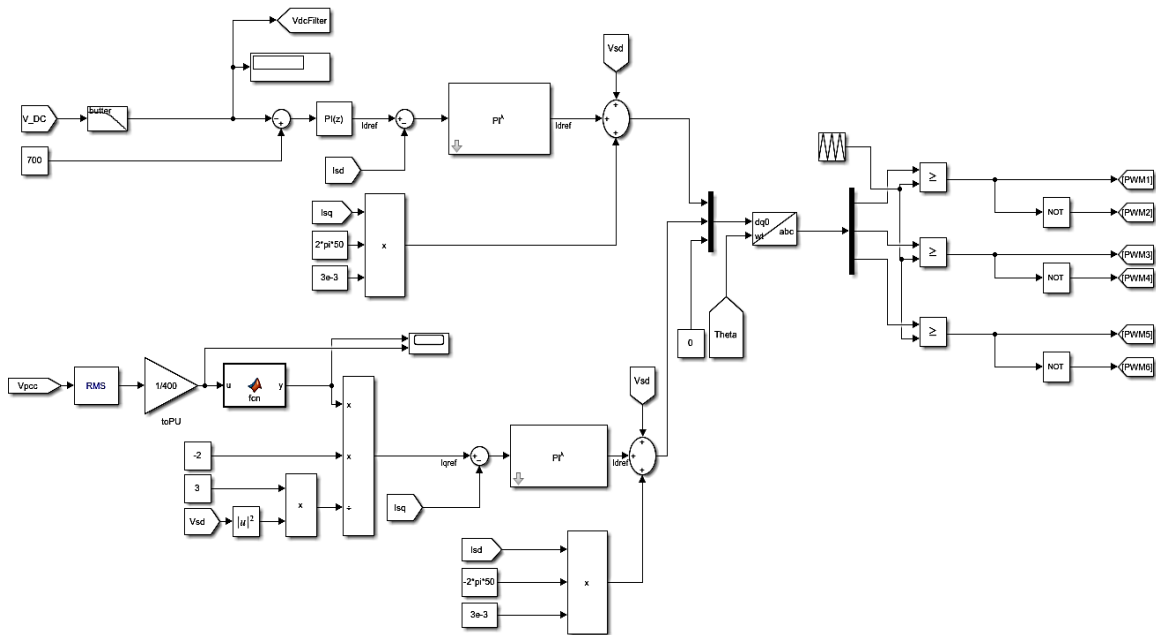


Figure 13. The MATLAB/Simulink circuit of the VSI controller

As was previously noted, the VSI controller requires the phase locked loop (PLL) control circuit in order to extract the phase of the grid voltage vector. Controlling grid-connected PV inverters relies heavily on knowing the phase angle of the grid power. Its functions include switching control of the inverter, determination of active and reactive power levels, and transformation of feedback variables into a frame appropriate for the chosen control strategy. Figure 14 depicts the PLL's corresponding Simulink model.

As shown previously in Figure 13, the Simulink model of the VSI controller. Two loops, an exterior voltage loop that controls the DC-link voltage and an internal current loop that controls the grid currents ( $I_d$  and  $I_q$ ), work together to accomplish the controller's goals. DC-link voltage controller outputs active current ( $I_d^{ref}$ ) reference. Depending on the fluctuations in PCC voltages, the  $Q(v)$  control mechanism is used to establish the reactive current reference ( $I_q^{ref}$ ). With the predicted phase angle of the grid voltages ( $\theta_s$ ), the grid voltages and currents ( $V_{abc}$ ,  $I_{abc}$ ) are translated into a dq frame that spins in synchrony with the grid voltage.  $V_{d,inv}$  and  $V_{q,inv}$  voltage outputs of the current controllers are utilized as a reference to the SPWM generator. To remove VSI-generated harmonics, a grid filter using a low-pass linear-comb (LCL) filter is developed and implemented. The calculated values of the filter parts are shown in Table 3 provides a concise summary of the intended performance of the LCL filter's individual parts.

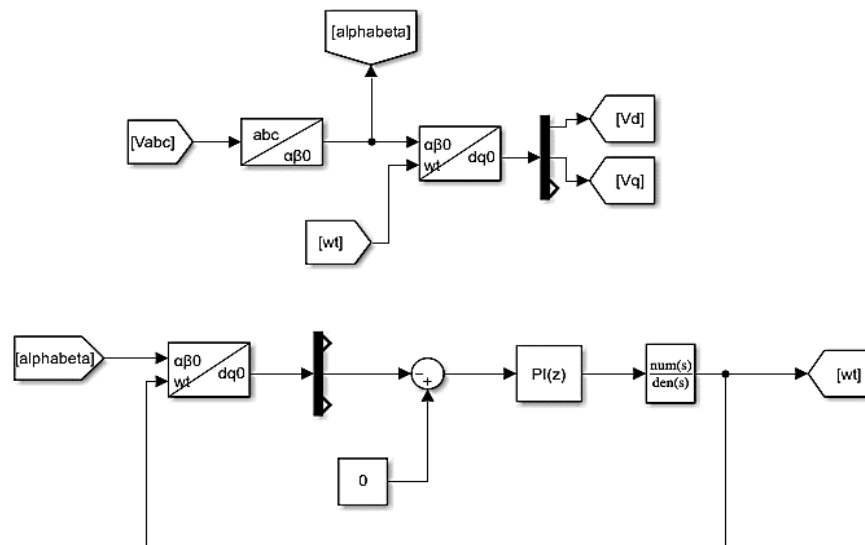


Figure 14. The MATLAB/Simulink circuit of PLL

Table 3. The designed LCL filter components value

Parameter	Value
$L_i$	0.0013 H
$C_f$	148.82 $\mu F$
$L_g$	386 $\mu H$
$R_{sd}$	1.4 $\mu$ ohm

The grid: the PV array is connected to 400  $V_{L-L}^{rms}$  grid line at 50 Hz frequency, and the local load: the PV array is supplying a local load with different values depends on the scenario; the required power needed for the load is consumed from the grid. At normal condition when there is no under or over voltage at PCC, the grid is supplying the load with all required reactive power.

**5.1. Optimized FOPI controller design**

The system the FOPI controller used to control active and reactive power at the outer control loop by comparing the grid currents with the reference currents. This control loop tries to keep the AC voltage at PCC nearest to the voltage of the grid as much as possible through an efficiently reactive power control for the PV inverter power. The performance of the FOPI controller compared with the performance of the traditional PI controller, when applied at the same system. The FOMCON toolbox for MATLAB used to design the FO-PI controller, which is a fractional-order calculus-based toolbox for system modeling and control design in addition to the traditional toolbox for design PI controllers. Salp swarm optimization algorithm is used as a tuning method to estimate the FO-PI and PI controller's parameters. In order to achieve this goal, the suggested

method employs ITAE as the fitness function. We write the code for the formulated FF and SSA technique. To determine FF, we bring the PCC rms voltage value,  $V_{Pcc}$ , from the MATLAB/Simulink into the MATLAB workspace and compare it to the reference voltage,  $V_{ref}$ . As shown in Figure 11, the SSA algorithm is used to reduce and evaluate the estimated optimum values of the FO-PI and PI controller parameters. The SSA algorithm was limited to no more than 200 iterations. Multiple simulation runs were needed for the dataset because of the random nature of SSA. Instead of using a physical search agent, the optimal values in this study are determined using a simulation search agent with a threshold of 20. In order to get the ideal settings for the FO-PI and PI controllers, an optimization issue has been given, as shown in Figure 15, and the suggested SSA has been used to solve this problem, as shown by the convergence behavior curve. It is clear that the FF value decreases as the number of iterations grows, hence minimizing the FF guarantees progress towards the ideal solution.

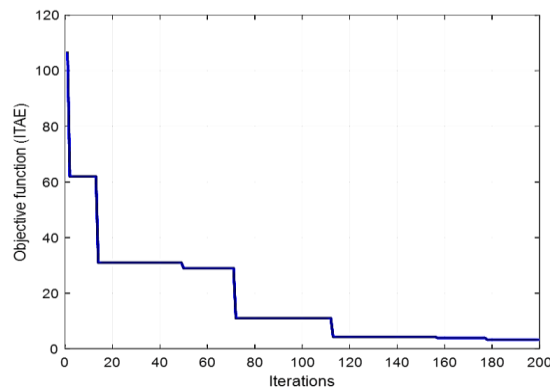


Figure 15. An illustration of the suggested SSA's convergence behavior curve in resolving the given optimization issue

The SSA optimization method, as shown in Figure 11, was obtained in the simulation's 177 iteration, lower limits of  $[K_p, K_i, \text{ and } \lambda]$  is  $[0 \ 0 \ 0]$  and upper limits  $[100 \ 100 \ 0.999]$ . The optimized gains of FO-PI controller ( $K_p, K_i, \text{ and } \lambda$ ) and PI controller ( $K_p$  and  $K_i$ ) were given as in Table 4. Finally, to compare the transient response of the system under different conditions, the optimized MATLAB parameters were imported into the Simulink FO-PI model and PI model. In this part of the study, various settings tested in the MATLAB/Simulink environment in order to see if the mentioned controller can be done with PV inverters in the electrical grid where a solar system is connected. The control system performance evaluated and compared with the traditional system, which depends on the PI controller. In these setting, the amount of radiation in the environment, grid voltage and change of grid reactive power modeled, and how the inverter responded to the grid in terms of active and reactive power were evaluated. The proposed control algorithm would be tested and simulated for these scenarios:

- Decreasing in solar radiation causes a decrease in the PV generation, which occurs in a situation of winter day where the grid enacted to under voltage due to low solar power production and high-power consumption.
- Increasing in the solar radiation causes an increase in the PV generation, which occurring in a situation of summer day where the grid enacted to over voltage situation due to high solar power production and low power consumption.

Because there are two terms (or parameters) in its construction, it is referred to as the "two modes controller." Each performance index has its own set of recommended values for these variables. The integral of square error between a measured process variable and a target value is one such measure of efficiency. The created controller is an effort toward reducing the integral of square error to boost dynamic responsiveness. Parameter values for both actions may be understood in terms of time: (P) is dependent on the error occurring at the moment, while (I) is dependent on the sum of all previous errors. When combined, they form what is known as the PI controller. Time response and stability of the system as a function of the parameters of each operation are discussed in [44].

## 5.2. PV generation decrease

In this scenario a decreasing in the radiation causes a decreasing in PV system generation less than the load consumption, then the load will consume the remains required active power from the grid, due to this changes a voltage drop  $\Delta V$  will be occur at PCC, and the voltage exceeds the grid code permissible limit of voltage. The voltage drop will add a negative reactive current to the grid through PCC. Therefore, positive

reactive current should be injected by the inverter. In other, word the inverter will generate and inject positive reactive power into the grid to compensate for the reactive power decreasing in the grid. Which leads to fixing the voltage at PCC. Table 5, shows the grid voltage permissible limit needed for Q(v) control method to decide the amount of reactive power that needs to be injected into the grid to fix PCC voltage. This method applied and used in MATLAB Coding and Simulink to determine the reference reactive current.

Table 4. The optimized controller’s parameters

Controller type	$K_p$	$K_i$	$\lambda$
PI	0.4613	0.0968	-
FOPI	0.6327	0.1172	0.8459

Table 5. Setting for PV inverter control

Method Q(v)	Method
[U1 U2 U3 U4]	[362 380 420 438]
$Q_{max}$ production	48.432Kvar at lagging power factor = 0.9

**5.3. The PV system generation decreases from 95 KW to 45 KW and the load is 100+j50 KVA**

The simulation results are shown in Figures 16 to 18. From the figures, it is possible to conclude that when the PV system generation decreases from 95 KW to 45 KW which covers 45% of load where the load will consume the rest 55% of its active power from the grid. This change leads to under voltage at PCC where  $V_{pcc}$  becomes 375 volts, ( $V_2 > V_{pcc} > V_1$ ) so the inverter injects about 13 KVAR into grid in order to fixing the voltage to almost 400 volt. Figure 17 shows the voltage and current of the inverter, it’s clear that the inverter voltage before the generation changes is in phase with current so which means that no reactive power injection by the inverter but when the generation decrease the inverter voltage is lagging the current which means that the inverter injected positive reactive power into the grid.

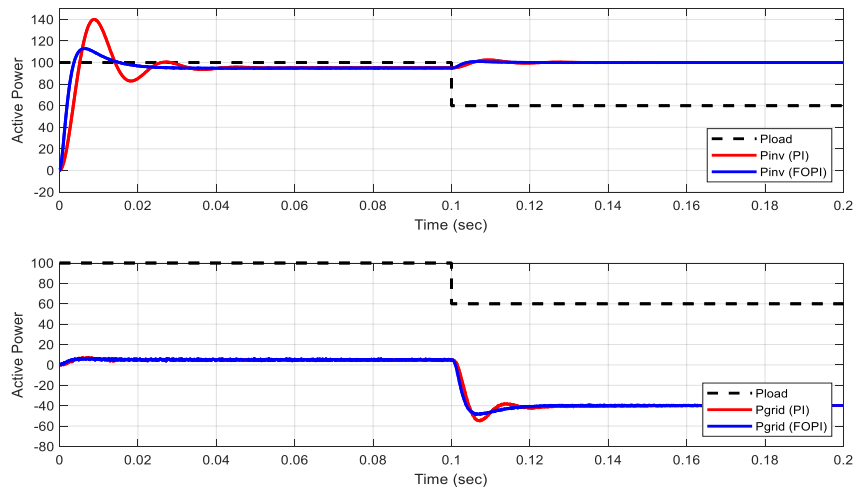


Figure 16. Scenario (II)-case 1: The active power of the inverter, grid, load, with FOPI VS PI controllers

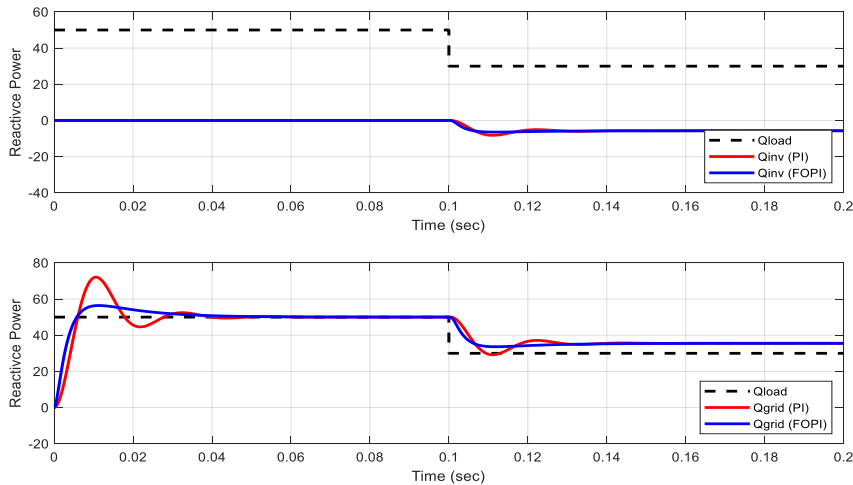


Figure 17. Scenario (II)-case 1: The reactive power of the inverter, grid, load, with FOPI VS PI controllers

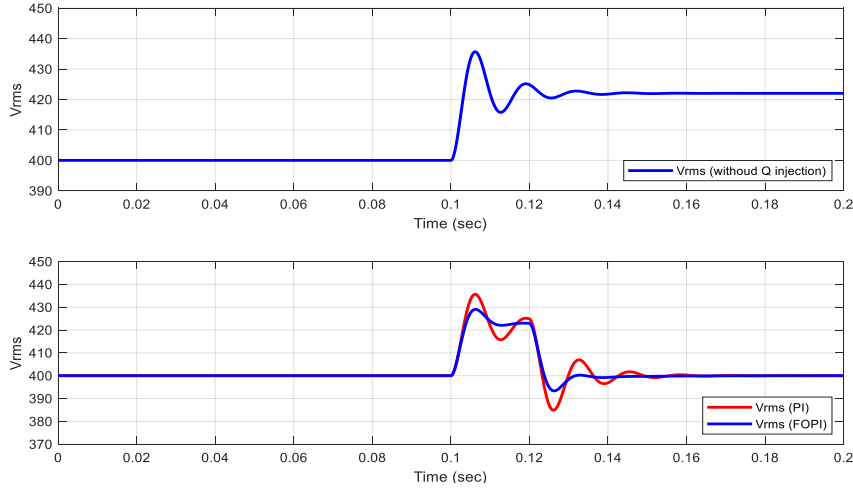


Figure 18. Scenario (II)-case 1: The voltage at PCC before Q injection and after Q injection with FOPI VS PI controllers

**5.4. The load decreased to 25+j15 KVA and the PV system generation increased to maximum generation 100 KW**

The simulation results are shown in Figures 19 to 21. From the figures, it is possible to conclude that when the load is decreased to 25 + j15 KVA and the PV system generation increased from 95 KW to 100 KW which covers 100% of load active power and the rest active power will have injected into the grid. This change leads to overvoltage at PCC where  $V_{pcc}$  becomes 441.43 volts, ( $V_{pcc} > V_4$ ) so the inverter in this case is absorbed from the grid the maximum possible amount of reactive power, which is about 48.4 KVAR as a result, the  $V_{pcc}$  decreased to almost 408 volts. it's clear that the inverter voltage before the generation changes is in phase with the current which means that no reactive power injection by the inverter but when the generation increase and load decrease, the inverter voltage is leading the current which means that the inverter injected negative reactive power into the grid. In the Table 6, we present the comparisons of the performance data of the proposed method and the traditional method.

Table 6. The performance comparison for the active power of grid

	Settling time (s)		Rising time (s)		Overshoot (100%)	
	PI	FOPI	PI	FOPI	PI	FOPI
Scenario (I)-case 1	0.0264	0.0229	0.0110	0.0086	63.4	18.2
Scenario (I)-case 2:	0.0253	0.0211	0.0042	0.0039	35.3	17.6
Scenario (II)-case 1:	0.0193	0.0178	0.0147	0.0126	37.8	25.1
Scenario (II)-case 2:	0.0185	0.0171	0.0056	0.0044	33.9	24.5

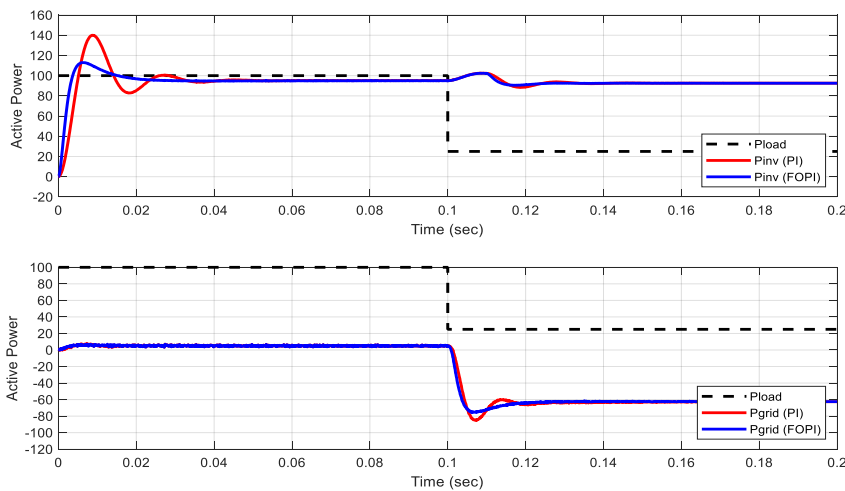


Figure 19. Scenario (II)-case 2: The active power of the inverter, grid, load, with FOPI VS PI controllers

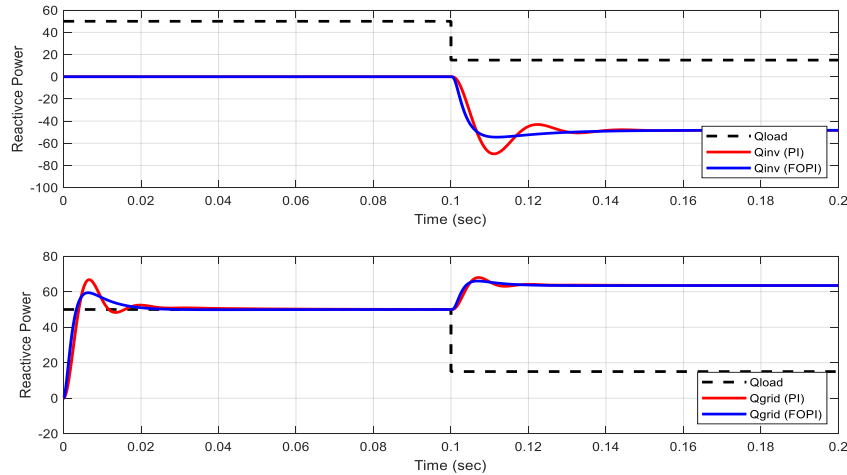


Figure 20. Scenario (II)-case 2: The reactive power of the inverter, grid, load, with FOPI VS PI controllers

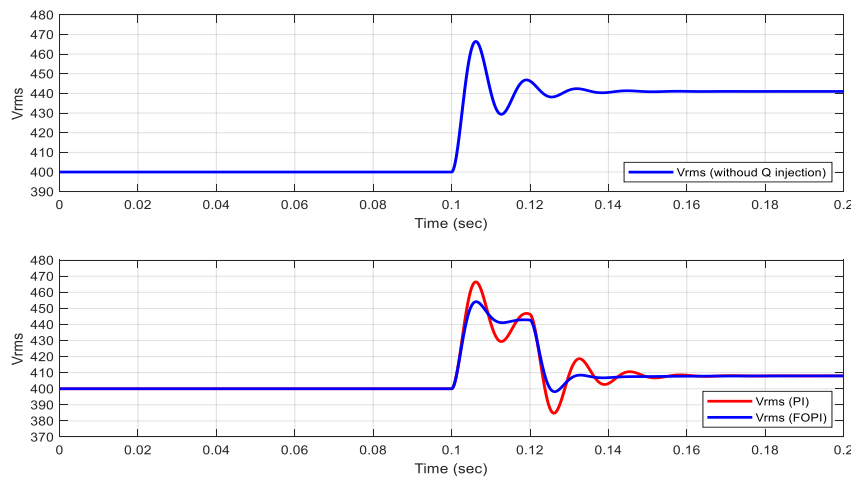


Figure 21. Scenario (II)-case 2: voltage at PCC before Q injection and after Q injection with FOPI VS PI controllers

## 6. CONCLUSION

A developed model for a two-stage grid-connected PV system is modeled and simulated using MATLAB/Simulink tools. The VSI control circuit, based on FOPI controllers and comparing their performance with traditional PI controllers. Salp swarm optimization algorithm SSA used to design the FOPI controller. Where the role of these controllers is to control the active and reactive power for solar inverters by utilizing the capability of these inverters to absorb and generate the reactive power, which may adjust the problem of the overvoltage and under-voltage and support the voltage in the point of common coupling PCC.

After modeling, testing, and validating the system. The whole photovoltaic array used to model many common situations across a range of grid and climate states. Simulation results in all applied scenarios shows that the FOPI controller give a better time response than the traditional PI controller. Where FOPI controllers in general shows faster time response since the time response was faster to reaching the steady state value (less settling time). In addition, the time response has less rising time, less peak time, and less percentage of overshoot, therefore less THD.

## REFERENCES




- [1] T. A. Jumani, M. W. Mustafa, M. M. Rasid, W. Anjum, and S. Ayub, "Salp swarm optimization algorithm-based controller for dynamic response and power quality enhancement of an islanded microgrid-," *Processes*, vol. 7, no. 11, 2019, doi: 10.3390/pr7110840.

- [2] M. Emarati, M. Barani, H. Farahmand, J. Aghaei, and P. C. del Granado, "A two-level over-voltage control strategy in distribution networks with high PV penetration," *International Journal of Electrical Power and Energy Systems*, vol. 130, 2021, doi: 10.1016/j.ijepes.2021.106763.
- [3] N. Bouderrès, D. Kerdoun, A. Djellad, S. Chiheb, and A. Dekhane, "Optimization of Fractional Order PI Controller by PSO Algorithm Applied to a Grid-Connected Photovoltaic System," *Journal Européen des Systèmes Automatisés*, vol. 55, no. 4, pp. 427–438, 2022, doi: 10.18280/jesa.550401.
- [4] R. Krishan, S. K. Singh, S. Patnaik, and S. Verma, "Reactive Power Control Strategies for Solar Inverters to Increase the Penetration Level of RE in Power Grid," *2nd International Conference on Large-Scale Grid Integration of Renewable Energy in India*, pp. 1–9, 2019.
- [5] S. Sharma *et al.*, "Modeling and sensitivity analysis of grid-connected hybrid green microgrid system," *Ain Shams Engineering Journal*, vol. 13, no. 4, 2022, doi: 10.1016/j.asej.2021.101679.
- [6] J. Huang, M. Liu, J. Zhang, W. Dong, and Z. Chen, "Analysis and field test on reactive capability of photovoltaic power plants based on clusters of inverters," *Journal of Modern Power Systems and Clean Energy*, vol. 5, no. 2, pp. 283–289, 2017, doi: 10.1007/s40565-015-0154-7.
- [7] S. Bhattacharyya, D. S. Kumar P, S. Samanta, and S. Mishra, "Steady output and fast tracking MPPT (SOFT-MPPT) for P&O and InC algorithms," *IEEE Transactions on Sustainable Energy*, vol. 12, no. 1, pp. 293–302, 2021, doi: 10.1109/TSTE.2020.2991768.
- [8] K. A. Tehrani, T. Capitaine, L. Barrandon, M. Hamzaoui, S. M. R. Rafiei, and A. Lebrun, "Current control design with a fractional-order PID for a three-level inverter," *Proceedings of the 2011 14th European Conference on Power Electronics and Applications, EPE 2011*, 2011.
- [9] M. Mao, L. Cui, Q. Zhang, K. Guo, L. Zhou, and H. Huang, "Classification and summarization of solar photovoltaic MPPT techniques: A review based on traditional and intelligent control strategies," *Energy Reports*, vol. 6, pp. 1312–1327, 2020, doi: 10.1016/j.egy.2020.05.013.
- [10] D. Almeida, J. Pasupuleti, and J. Ekanayake, "Comparison of reactive power control techniques for solar pv inverters to mitigate voltage rise in low-voltage grids," *Electronics (Switzerland)*, vol. 10, no. 13, 2021, doi: 10.3390/electronics10131569.
- [11] S. Kakkar *et al.*, "Design and Control of Grid-Connected PWM Rectifiers by Optimizing Fractional Order PI Controller Using Water Cycle Algorithm," *IEEE Access*, vol. 9, pp. 125941–125954, 2021, doi: 10.1109/ACCESS.2021.3110431.
- [12] C. Bao, X. Ruan, X. Wang, W. Li, D. Pan, and K. Weng, "Step-by-step controller design for LCL-Type Grid-Connected inverter with capacitor-current-feedback active-damping," *IEEE Transactions on Power Electronics*, vol. 29, no. 3, pp. 1239–1253, 2014, doi: 10.1109/TPEL.2013.2262378.
- [13] V. R. Chowdhury, "Internal Model Based Grid Voltage Estimation and Control of a Three-Phase Grid Connected Inverter for PV Application," *IEEE Transactions on Energy Conversion*, vol. 36, no. 4, pp. 3568–3577, 2021, doi: 10.1109/TEC.2021.3079908.
- [14] Y. Jia, J. Zhao, and X. Fu, "Direct grid current control of LCL-filtered grid-connected inverter mitigating grid voltage disturbance," *IEEE Transactions on Power Electronics*, vol. 29, no. 3, pp. 1532–1541, 2014, doi: 10.1109/TPEL.2013.2264098.
- [15] Y. Zhang, J. Liu, H. Yang, and J. Gao, "Direct Power Control of Pulsewidth Modulated Rectifiers Without DC Voltage Oscillations under Unbalanced Grid Conditions," *IEEE Transactions on Industrial Electronics*, vol. 65, no. 10, pp. 7900–7910, 2018, doi: 10.1109/TIE.2018.2807421.
- [16] S. K. Sampangi and J. Thangavelu, "Optimal allocation of renewable distributed generation and capacitor banks in distribution systems using salp swarm algorithm," *International Journal of Renewable Energy Research*, no. March, pp. 96–107, 2019.
- [17] G. Yang *et al.*, "Direct power control of three-level NPC grid-connected system combined with fault-tolerant technology," *Microelectronics Reliability*, vol. 88–90, pp. 1057–1062, 2018, doi: 10.1016/j.microrel.2018.07.140.
- [18] A. A. Abusnaina, S. Ahmad, R. Jarrar, and M. Mafarja, "Training neural networks using Salp Swarm Algorithm for pattern classification," *ACM International Conference Proceeding Series*, 2018, doi: 10.1145/3231053.3231070.
- [19] S. Ouchen, H. Steinhart, M. Benbouzid, and F. Blaabjerg, "Robust DPC-SVM control strategy for shunt active power filter based on  $H_{\infty}$  regulators," *International Journal of Electrical Power and Energy Systems*, vol. 117, 2020, doi: 10.1016/j.ijepes.2019.105699.
- [20] H. Faris, S. Mirjalili, I. Aljarah, M. Mafarja, and A. A. Heidari, "Salp swarm algorithm: Theory, literature review, and application in extreme learning machines," *Studies in Computational Intelligence*, vol. 811, pp. 185–199, 2020, doi: 10.1007/978-3-030-12127-3\_11.
- [21] G. Lorenzini, M. A. Kamarposhti, and A. A. Ahmed Solymán, "Optimization of PID controller parameters for automatic generation control in two-area heating system using firefly algorithm," *International Journal of Safety and Security Engineering*, vol. 11, no. 3, pp. 213–222, 2021, doi: 10.18280/ijss.110301.
- [22] S. M. A. Altbawi, A. S. Bin Mokhtar, T. A. Jumani, I. Khan, N. N. Hamadneh, and A. Khan, "Optimal design of Fractional order PID controller based Automatic voltage regulator system using gradient-based optimization algorithm," *Journal of King Saud University - Engineering Sciences*, 2021, doi: 10.1016/j.jksues.2021.07.009.
- [23] H. Erol, "Stability analysis of pitch angle control of large wind turbines with fractional order PID controller," *Sustainable Energy, Grids and Networks*, vol. 26, 2021, doi: 10.1016/j.segan.2021.100430.
- [24] A. Jain and R. Saravanakumar, "Comparative analysis of fractional order PI and integer order PI based controller for hybrid standalone wind energy conversion system," *Environmental Progress and Sustainable Energy*, vol. 39, no. 2, 2020, doi: 10.1002/ep.13293.
- [25] M. S. Ayas and E. Sahin, "FOPID controller with fractional filter for an automatic voltage regulator," *Computers and Electrical Engineering*, vol. 90, 2021, doi: 10.1016/j.compeleceng.2020.106895.
- [26] O. Karahan, "Design of optimal fractional order fuzzy PID controller based on cuckoo search algorithm for core power control in molten salt reactors," *Progress in Nuclear Energy*, vol. 139, 2021, doi: 10.1016/j.pnucene.2021.103868.
- [27] W. Fu, K. Wang, C. Li, and J. Tan, "Multi-step short-term wind speed forecasting approach based on multi-scale dominant ingredient chaotic analysis, improved hybrid GWO-SCA optimization and ELM," *Energy Conversion and Management*, vol. 187, pp. 356–377, 2019, doi: 10.1016/j.enconman.2019.02.086.
- [28] Z. Wang, Y. Yu, W. Gao, M. Davari and C. Deng, "Adaptive, Optimal, Virtual Synchronous Generator Control of Three-Phase Grid-Connected Inverters Under Different Grid Conditions—An Adaptive Dynamic Programming Approach," in *IEEE Transactions on Industrial Informatics*, vol. 18, no. 11, pp. 7388–7399, Nov. 2022, doi: 10.1109/TII.2021.3138893.
- [29] Z. Albataineh, K. F. Hayajneh, H. Shakhtrah, R. Al Athamneh, and M. Anan, "Channel estimation for reconfigurable intelligent surface-assisted mmWave based on Rényi entropy function," *Scientific reports*, vol. 12, no. 1, p. 22301, 2022, doi: 10.1038/s41598-022-26672-3.
- [30] R. Celikel, M. Yilmaz, and A. Gundogdu, "A voltage scanning-based MPPT method for PV power systems under complex partial shading conditions," *Renewable Energy*, vol. 184, pp. 361–373, 2022, doi: 10.1016/j.renene.2021.11.098.




- [31] K. Zeb *et al.*, "Faults and Fault Ride Through strategies for grid-connected photovoltaic system: A comprehensive review," *Renewable and Sustainable Energy Reviews*, vol. 158, 2022, doi: 10.1016/j.rser.2022.112125.
- [32] A. I. M. Ali and H. R. A. Mohamed, "Improved P&O MPPT algorithm with efficient open-circuit voltage estimation for two-stage grid-integrated PV system under realistic solar radiation," *International Journal of Electrical Power and Energy Systems*, vol. 137, 2022, doi: 10.1016/j.ijepes.2021.107805.
- [33] H. Li, B. Song, X. Tang, Y. Xie, and X. Zhou, "Controller optimization using data-driven constrained bat algorithm with gradient-based depth-first search strategy," *ISA Transactions*, vol. 125, pp. 212–236, 2022, doi: 10.1016/j.isatra.2021.06.032.
- [34] S. Obukhov, A. Ibrahim, A. A. Zaki Diab, A. S. Al-Sumaiti, and R. Aboelsaud, "Optimal Performance of Dynamic Particle Swarm Optimization Based Maximum Power Trackers for Stand-Alone PV System under Partial Shading Conditions," *IEEE Access*, vol. 8, pp. 20770–20785, 2020, doi: 10.1109/ACCESS.2020.2966430.
- [35] N. Khodadadi, L. Abualigah, E. -S. M. El-Kenawy, V. Snasel and S. Mirjalili, "An Archive-Based Multi-Objective Arithmetic Optimization Algorithm for Solving Industrial Engineering Problems," in *IEEE Access*, vol. 10, pp. 106673-106698, 2022, doi: 10.1109/ACCESS.2022.3212081.
- [36] Z. Albataineh, "Low-Complexity Near-Optimal Iterative Signal Detection Based on MSD-CG Method for Uplink Massive MIMO Systems," *Wireless Personal Communications*, vol. 116, no. 3, pp. 2549–2563, 2021, doi: 10.1007/s11277-020-07810-4.
- [37] Z. Albataineh, "Blind Decoding of Massive MIMO Uplink Systems Based on the Higher Order Cumulants," *Wireless Personal Communications*, vol. 103, no. 2, pp. 1835–1847, 2018, doi: 10.1007/s11277-018-5883-2.
- [38] Z. Albataineh, N. Al-Zoubi, and A. Musa, "Channel estimation for massive MIMO system using the shannon entropy function," *Cluster Computing*, 2022, doi: 10.1007/s10586-022-03783-0.
- [39] W. Aribowo, Supari, and B. Suprianto, "Optimization of PID parameters for controlling DC motor based on the aquila optimizer algorithm," *International Journal of Power Electronics and Drive Systems*, vol. 13, no. 1, pp. 216–222, 2022, doi: 10.11591/ijpeds.v13.i1.pp216-222.
- [40] M. S. Amiri, M. F. Ibrahim, and R. Ramli, "Optimal parameter estimation for a DC motor using genetic algorithm," *International Journal of Power Electronics and Drive Systems*, vol. 11, no. 2, pp. 1047–1054, 2020, doi: 10.11591/ijpeds.v11.i2.pp1047-1054.
- [41] S. J. Hammoodi, K. S. Flayyih, and A. R. Hamad, "Design and implementation speed control system of DC motor based on PID control and matlab simulink," *International Journal of Power Electronics and Drive Systems*, vol. 11, no. 1, pp. 127–134, 2020, doi: 10.11591/ijpeds.v11.i1.pp127-134.
- [42] B. A. Obaid, A. L. Saleh, and A. K. Kadhim, "Resolving of optimal fractional PID controller for DC motor drive based on anti-windup by invasive weed optimization technique," *Indonesian Journal of Electrical Engineering and Computer Science*, vol. 15, no. 1, pp. 95–103, 2019, doi: 10.11591/ijeecs.v15.i1.pp95-103.
- [43] R. Çelikel and M. Özdemir, "A method for current control of the flywheel energy storage system used in satellites," *Tehnicki Vjesnik*, vol. 26, no. 3, pp. 631–638, 2019, doi: 10.17559/TV-20160328090219.
- [44] S. Noureddine, S. Morsli, A. Tayeb, and D. Mouloud, "Optimal Fractional-Order PI Control Design for a Variable Speed PMSG-Based Wind Turbine," *Journal Europeen des Systemes Automatises*, vol. 54, no. 6, pp. 915–922, 2021, doi: 10.18280/jesa.540615.
- [45] N. Altin, S. Ozdemir, M. Khayamy and A. Nasiri, "A Novel Topology for Solar PV Inverter Based on an LLC Resonant Converter With Optimal Frequency and Phase-Shift Control," in *IEEE Transactions on Industry Applications*, vol. 58, no. 4, pp. 5042–5054, July-Aug. 2022, doi: 10.1109/TIA.2022.3163372.
- [46] A. Gundogdu, "System Identification Based ARV-MPPT Technique for PV Systems Under Variable Atmospheric Conditions," *IEEE Access*, vol. 10, pp. 51325–51342, 2022, doi: 10.1109/ACCESS.2022.3174107.
- [47] R. Celikel and A. Gundogdu, "System identification-based MPPT algorithm for PV systems under variable atmosphere conditions using current sensorless approach," *International Transactions on Electrical Energy Systems*, vol. 30, no. 8, 2020, doi: 10.1002/2050-7038.12433.
- [48] M. A. Al-Tahat, "Optimization of fractional order PI CONTROLLER TO REGULATE VOLTAGE OF GRID CONNECTED PHOTOVOLTAIC SYstem," Thesis, Yarmouk University, 2021.

## BIOGRAPHIES OF AUTHORS






**Ibrahim Altawil**    was born in Ramallah, Jordan. University Collage of Swansea, Wales, UK, 1996, Electrical Engineering. Now he is associate professor Department of Electrical Power Engineering Haijjawi Faculty for Engineering Technology, Yarmouk University-Jordan. His current research interests include power electronics applied to photovoltaic, renewable energy, and engineering education their application. He can be contacted at email: ialtawil@yu.edu.jo






**Mohammad Awad Momani**    Associate Professor of Electrical Power Engineering EPE, Yarmouk University. He grew up in the city of Al-Nueimah in Jordan. He is now an associate professor at Yarmouk University in Jordan, department of electrical power engineering of Haijjawi Faculty of Engineering Technology. Power system planning, Power electronics, renewable energy, and their application to electrical power engineering education are all areas of focus for his present research. He can be contacted at email: mohammadh@yu.edu.jo.








**Mahmood A. Al-Tahat**    is a control engineer at National Electric Power Co (NEPCO), Jordan. Who has a Master's degree in electrical and power engineering from Yarmouk University. His current research focuses specifically on electrical power systems control. He can be contacted at email: mthat1985@gmail.com.






**Raed Al Athamneh**    is currently an assistant professor and an assistant dean at the deanship of academic development and international outreach at The Hashemite University. He received the bachelor's degree in industrial engineering from Jordan University of Science and Technology, Irbid, Jordan in 2009 and the master's degree from University of Jordan, Amman, Jordan in 2015. He completed a masters and a Ph.D. degree in industrial systems engineering from Auburn university, Auburn, Alabama, USA in 2018 and 2020, respectively. His research interests include reliability modelling, and fatigue analysis, microelectronic reliability and optimization in manufacturing and service systems. He can be contacted at email: raedq@hu.edu.jo



**Mohammed Adnan Al-Saadi**    was born in Dubai, UAE, in 1986. He received the B.S. degree in electrical power engineering from Yarmouk University, Jordan, in 2010. He received the M.S. degree in electrical power engineering from Yarmouk University, Jordan, in 2019. From 2010 to 2011, he was a Research engineer in energy flow consulting company. Since 2011, he has been a laboratory instructor with the electrical power Engineering Department, Yarmouk university. His research interests include economic dispatch and optimal power flow for power system grid, FOPID applications, Load Forecasting, optimization and deep learning. He can be contacted at email: saedi@yu.edu.jo.



**Zaid Albataineh**    received the B.S. degree in electrical engineering from the Yarmouk University, Irbid, Jordan, in 2006, and received the M.S. degree in the communication and electronic engineering from the Jordan University of Science and Technology JUST, Irbid, Jordan, in 2009. He received the Ph.D. degree in electrical and computer engineering department, Michigan State University (MSU), USA, in 2014. His research interests include Blind Source Separation, Independent Component analysis, Nonnegative matrix Factorization, Wireless Communication, DSP Implementation, VLSI, Analog Integrated Circuit and RF Integrated Circuit. He can be contacted at email: zaid.bataneh@yu.edu.jo.